Laser Doppler thermometry in flat flames

Combust. Sci. and Tech., 1994, Vol. 99, pp. 105–118
Photocopying permitted by license only

Laser Doppler Thermometry in Flat Flames

A. Van MAAREN, and L. P. H. de GOEY *Eindhoven University of Technology, Faculty of Mechanical Engineering, P.O. Box 513, 5600 MB Eindhoven, The Netherlands*

(Received July 27, 1993)

ABSTRACT—Laser Doppler Velocimetry measurements are performed in flat flames, stabilized on a newly developed flat-flame burner. It is shown that the velocity component perpendicular to the main flow direction, induced by expansion in the reaction zone and buoyancy in the burnt gas, is significant. A method is derived with which the temperature profile of flat flames can be determined from two-dimensional Laser Doppler Velocimetry measurements. Good agreement is found when compared to one-dimensional flame calculations and experimental data obtained from the literature. A method is presented to describe the influence of expansion and buoyancy on the burnt gas flow.

Key Words: Velocity measurements, temperature measurements, laminar flames, one-dimensional flames, Laser Doppler Velocimetry

LIST OF SYMBOLS

a	Constant	arbitrary units
β	Buoyancy index	–
c_r	Axial dependence of the radial velocity	s^{-1}
ϕ	Equivalence ratio	–
g	Gravitational constant	$m.s^{-2}$
$\mathscr{G}$	Constant	$m.s^{-2}$
K	Average molar mass correction factor	–
ξ	Integration variable	m
M	Average molar mass	$kg.\ mol^{-1}$
P, p	Pressure	$kg.m^{-1}.\ s^{-2}$
r	Radial coordinate	m
$\mathscr{R}$	Universal gas constant	$m^2 \cdot s^{-2}.K^{-1}$
R	Constant	m
ρ	Mass density	$kg.m^{-3}$
T	Temperature	K
u	Axial velocity	$m.s^{-1}$
U	Average unburnt gas velocity	$m.s^{-1}$
v	Radial velocity	$m.s^{-1}$
x	Axial coordinate	m

Subscripts

g	Unburnt gas
b	Burnt gas

INTRODUCTION

The one-dimensional (1-D) flame is one of the most studied objects in laminar combustion research. One of the reasons is that numerical calculations of 1-D flames are relatively easy to perform. Furthermore, properties like burning velocity and flame temperature are defined unambiguously only in 1-D flames, since air entrainment, stretch or heat loss to the environment do not have to be taken into account. Nevertheless, comparison with experimental data is not self-evident. In practice, a flame that is assumed to be 1-D, the flat flame, suffers from several more-dimensional effects, which makes comparison with perfectly 1-D calculations still a delicate task. In particular, one of the important requirements for a flat flame is that the velocity profile of the unburnt gas is uniform. However, although much work has been done on measurements in flat flames, this has never been thoroughly investigated.

Velocities in a flat flame are interesting in itself, since there exists a direct relationship between the temperature and the velocity of a perfectly 1-D flame, which can be shown by the following analysis. Conservation of mass in a 1-D flow system yields:

$$\frac{\partial(\rho u)}{\partial x} = 0 \tag{1}$$

in which ρ is the mass density and u the velocity in the x-direction, perpendicular to the flat flame. The mass density can be related to the temperature T with the ideal gas law:

$$P = \frac{\rho \mathscr{R} T}{M} \tag{2}$$

in which M is the average molar mass of the mixture, and $\mathscr{R}$ is the universal gas constant. The pressure P may assumed to be constant in low Mach number hydrocarbon deflagration processes. When M is constant, combination of Equations (1) and (2) leads to the relation:

$$\frac{u}{T} = \frac{u_g}{T_g} \tag{3}$$

in which u_g is the unburnt gas velocity and T_g the unburnt gas temperature, equal to the ambient temperature of 298 K. With Equation (3), measurement of $u(x)$ suffices to calculate $T(x)$. Therefore, a 1-D flame offers the unique opportunity to measure in directly the temperature profile through measurement of the velocity profile. While temperature measurements are often difficult to perform accurately, velocity measurements with the Laser Doppler Velocimetry (LDV) technique can be performed with a high accuracy (the theoretical error is about 1%). Therefore, it is interesting to investigate whether Equation (3) can be applied to determine temperature profiles of flat flames.

LDV techniques have found widespread applications in laminar flames. However, the most widely used flat flame burner, the porous plug burner (see e.g., Botha and Spalding (1954)) can not be used for LDV experiments. The plug of the burner, which is essential to provide a uniform velocity profile, would be choked by the seeding particles necessary for the LDV system. Therefore, to be able to investigate the velocity profile of flat flames, we have developed a new flat flame burner, a perforated plate burner, which is particularly suited for LDV measurements. This burner has been introduced previously by van Maaren *et al.* (1994). Here we will discuss some features related with

its applicability to LDV measurements. We will present results of LDV measurements in both the unburnt and the burnt gas flow, which show that the velocity profile of a flat flame is never perfectly 1-D. There is always a velocity component perpendicular to the x-direction, due to expansion and buoyancy. Still, it is possible to relate the temperature to the velocity. We will present a method to determine the temperature profile of a flat flame from 2-D velocity measurements, that gives excellent results. Furthermore, we will present a simple model for describing expansion and buoyancy in the burnt gas flow in these flat flames, in order to assess the influence of the burner diameter and the flame temperature on the velocity profile.

THE PERFORATED PLATE BURNER

In Figure 1 the geometry of the flat flame burner is shown. The flame-stabilizing surface is a brass plate of 2 mm thickness and 30 mm diameter, perforated with a hexagonal pattern of small holes of 0.5 mm diameter and 0.7 mm pitch. The burner head is assembled on a plenum chamber, to provide a uniform velocity profile under the burner plate. The edge of the burner plate is maintained at a constant temperature by means of a cooling jacket. Additional cooling by means of an internal cooling coil, which is often employed in the case of porous plug burners, can not be used.

The temperature at which the burner plate edge is maintained is always higher than the initial gas temperature. One of the reasons is that applying a higher cooling temperature increases the stability of the flame, especially when operating near the adiabatic burning velocity. This principle is discussed by de Goey *et al.* (1993). The main reason to do this here is that condensating water vapor on a cold burner plate traps seeding particles, which eventually distorts the flow. The cooling temperature during the measurements was either 323 or 363 K. As a consequence, the entire burner increased in temperature, including the plenum chamber. To prevent the unburnt gas from being heated (thereby increasing T_g), the plenum chamber is cooled separately at a temperature of 298 K.

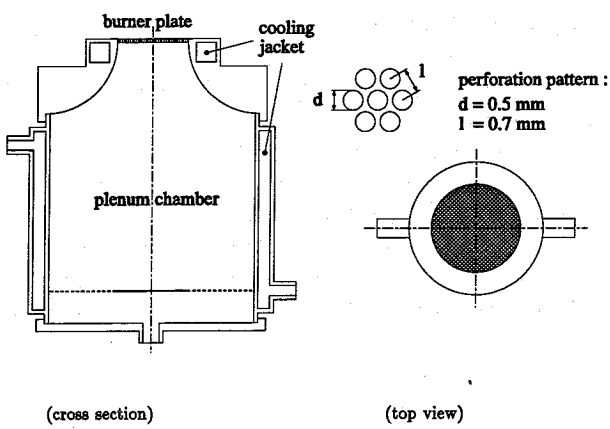

FIGURE 1 The perforated plate burner

Inevitably, both velocity and temperature boundary layers will exist, inside the burner and near the edge of the burner plate at exit of the burner. Consequently, all the measurements and the analysis must be restricted to a certain core region of the flow, where both the velocity and the temperature profile are uniform, i.e., where u and ρ are only dependent on x. As a result of the presence of the boundary layers the unburnt gas velocity u_g in the core region will not be equal to the average unburnt gas velocity U, defined as the volume flow rate (at ambient temperature and pressure) divided by the burner plate area. As will become clear in the next section, u_g is an important variable, which must be known accurately. Therefore, although the difference between U and u_g is usually less than 0.5 cm/s, still u_g is calibrated as function of U by LDV measurements. All the results presented in this paper are corrected through this calibration.

It must be anticipated that cooling at the edge of the burner plate may cause distortion of the radial velocity and temperature profile of the flame. Fox and Kihara (1972), Pritchard *et al.* (1972) and Kihara *et al.* (1975) investigated this theoretically in the case of a porous plug burner. Because the flame loses heat to the burner surface, edge cooling will result in a radial temperature profile in the burner plate. As the unburnt gas flowing through the plug practically attains the same temperature as the local plug temperature, a non-uniform radial temperature profile will be established in the unburnt gas, with possibly a temperature variation of 100 K or more. Because of the temperature dependence of the mass density and viscosity of the gas this may result in variation of u_g of more than 30%. This suggests that an initially flat velocity profile when the flame is absent will be distorted when the flame is present.

However, it is likely that in the case of the perforated plate burner the velocity profile of the burnt gas is not as much distorted as suggested. First of all, the thermal conductivity of the perforated plate is much higher than that of the porous plug. As a consequence, the maximum temperature variation in the plate is smaller, typically 20 K in the core region (see Van Maaren *et al.* (1994)). Besides, the plate is relatively thin compared to a porous plug (2 mm for the perforated plate, 1–3 cm for a porous plug). Therefore, the unburnt gas can not attain the same temperature in the case of a performed plate burner. Finally, the flame induces an extra pressure drop, which implies that the velocity variations will be smaller after the flame, as the results will show.

TEMPERATURE CALCULATION

In an ideal 1-D flame only one (axial) velocity component will be present. In a rotationally symmetric flat flame however, also a radial velocity component will appear. In the reaction zone the expansion of the gas also occurs in radial direction, inducing a positively orientated radial velocity. Furthermore, the hot combustion gas in a colder environment will be accelerated in axial direction due to buoyancy. To satisfy conservation of mass, a negatively orientated radial velocity component must appear. Therefore, Equation (3) is not appropriate as velocity-temperature relationship in practical flat flames. Instead, consider the stationary 2-D conservation of mass Equation in cylindrical coordinates:

$$\frac{1}{r}\frac{\partial(\rho v r)}{\partial r} + \frac{\partial(\rho u)}{\partial x} = 0. \tag{4}$$

As u and ρ are independent of r in the core region, Equation (4) can be integrated with respect to r to give an expression for the radial velocity component $v(x,r)$:

$$v(x,r) = -\frac{r}{2\rho}\frac{\partial(\rho u)}{\partial x} = c_r(x)\cdot r \tag{5}$$

where $v(x,0) = 0$ is used for reasons of symmetry. c_r is introduced because this quantity is easily determined through measurement of the radial velocity. Equation (5) indicates that v is linearly dependent on r.

Although M is practically constant in some cases (e.g., lean methane/air mixtures), in general M is not constant. This has to be taken into account in Equation (2) to relate the density with the temperature. If the temperature of the mixture changes from T_g to the flame temperature $T(x_b) = T_b$, M changes accordingly from M_g to M_b. Without the necessity to know the chemical composition of the gas mixture at every position x, to a good approximation $M(x)$ can be written as:

$$M(x) = \begin{cases} M_g + [M_b - M_g]\cdot\dfrac{T(x) - T_g}{T_b - T_g} & \text{for } x \le x_b \\ M_b & \text{for } x > x_b. \end{cases} \tag{6}$$

The validity of this approximation will be shown when the results are discussed. With Equation (6) a correction factor $K(x)$ can be defined as:

$$K(x) = \frac{M_g}{M(x)} \tag{7}$$

Substitution of Equations (2), (5)–(7) in Equation (4) and integrating with respect to x yields:

$$\frac{u(x)}{T(x)K(x)} = \frac{u_g}{T_g} - \int_0^x \frac{2c_r(\xi)d\xi}{T(\xi)K(\xi)} \tag{8}$$

in which subscript g denotes $x = 0$. An implicit expression for $T(x)$ is obtained, with an additional term compared to Equation (3) to take into account the radial velocity component. It appears that experimental data of both the axial velocity $u(x)$ and the radial velocity $v(x,r)$ yielding $c_r(x)$ is necessary to evaluate Equation (8), assuming that T_g, u_g, M_g and M_b are known. It can be seen that an error in either T_g or u_g causes a significant error in $T(x)$. Errors in $v(x,r)$ are less significant, as c_r appears only in the integral, which has a relative contribution of about 10% compared to the term u_g/T_g.

EXPERIMENTAL SETUP

The velocity is measured using a one-component LDV system, consisting of a 35 mW He-Ne laser, optics containing a beam splitter, a Bragg Cell and a focussing lens, Counter, Frequency Shifter, and photomultiplier. We use 1 μm Al_2O_3 particles as seeding, which are supplied to the unburnt gas flow by means of a small fluidized bed. Micrometer translation stages are used to translate the burner with respect to the measurement volume, which is 0.1 mm wide. This yields a good spatial resolution, which is necessary due to the steep velocity gradients in the flow.

Since we must measure two velocity components, while we have only a one-component system available, we measure both velocity components separately, with the optics rotated over an angle of 90° for the radial velocity component.

The burner is operated inside a ventilated chamber of about 1 m^3, to minimize the influence of draught.

The average unburnt gas velocity U and the equivalence ratio ϕ are adjusted by Mass Flow Controllers, which after calibration have an absolute error of less than 0.5%.

RESULTS

First, we investigate to what extent the flat flame burner produces flames in accordance with the previously mentioned assumptions. For this purpose profiles of the axial velocity were measured, of the unburnt gas and of the burnt gas, and also profiles of the radial velocity. These measurements were all performed using a methane/air mixture with $\phi = 0.8$, for various values of U. The effect of expansion and buoyancy is determined by measurement of the burnt gas acceleration and c_r. Finally, the temperature is calculated from these measurement. This is performed for various values of U, with $\phi = 0.8$, 1.2 and 1.4. The temperature results will be compared to 1-D flame calculations and experimental results found in the literature.

Axial velocity

In Figure 2a some results are shown of measurement of the unburnt gas velocity u_g without combustion, at a distance $x = 3$ mm above the burner plate, for various values

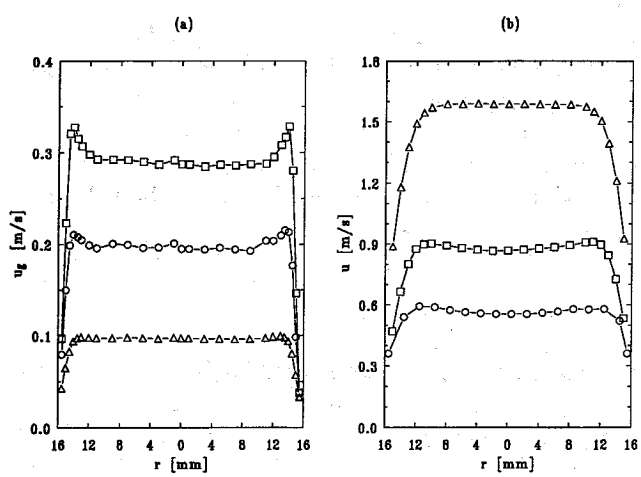

FIGURE 2a, b a. The velocity of the unburnt gas u_g as function of r, at $x = 3$ mm, for $U = 0.1$, 0.2 and 0.3 m/s; b. The axial velocity component of the burnt gas u as function of r, at $x = 3$ mm, for $U = 0.1$, 0.15 and 0.25 m/s

of U. It can be concluded that the maximum velocity variations in a core region of about 20 mm wide are 1–2%. However, for increasing U the boundary layers are distorted. These distortions are caused by the shape of the plenum chamber. Inserting for instance glass beads or wire gauze in the plenum chamber would probably remove the distortions, but would also cause seeding choking. We have not pursued this option, because the distortions are located outside the core region, and appeared to have no observable effect on the burnt gas velocity profile.

This can be seen in Figure 2b, where the axial velocity of the burnt gas is shown, at $x = 3$ mm. For $U = 0.25$ m/s we find a profile which is perfectly uniform in the core region. Comparison of Figure 2a and 2b shows, that the velocity variations are indeed smaller after the flame, which confirms the earlier statement concerning the pressure drop over the flame. For $U = 0.1$ and 0.15 m/s we find a distorted profile, with a velocity variation of about 5%. This is the effect caused by the non-uniform temperature profile of the unburnt gas, due to the burner plate edge cooling. For $U = 0.25$ m/s this is not found, because this velocity is close to the adiabatic burning velocity, where the heat loss of the flame is small. From the measurements it is concluded that when the maximum burner plate temperature variation in the core region smaller than 10 K, it has a negligible effect on the burnt gas velocity profile.

Radial velocity

Although the edge cooling of the burner plate can have an effect on the shape of the axial velocity profile of the burnt gas, it has no observable effect on the shape of the radial velocity profile. This is shown in Figure 3a. Here the radial velocity profile is shown for $U = 0.1$ m/s, at $x = 2$ and 4 mm. Clearly seen is the linear relationship between the radial velocity and radius in the core region. Measurement of the radial

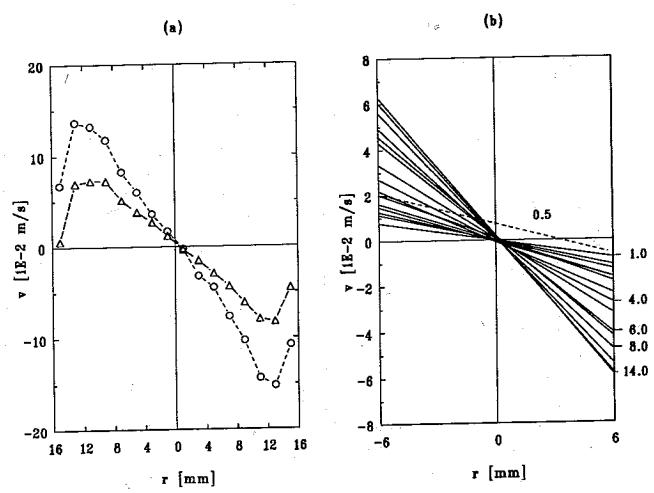

FIGURE 3a, b a. The radial velocity component of the burnt gas v as function of r, for $U = 0.1$ m/s, makers: $\triangle x = 2$ mm, $\circ x = 4$ mm; b. The radial velocity component of the burnt v gas for $x = 0.5$ to 14 mm, at $r = 6$ mm on either side of the burner centerline, with $U = 0.25$ m/s

velocity profile in any other case gives the same result. Therefore, these results confirm the prediction of Equation (5).

Another aspect that can be investigated is the symmetry of the flow. In Figure 2b no asymmetry can be observed. In Figure 3b the development of the radial velocity as function of x is shown, with $x = 0.5$ to 14 mm, for $U = 0.25$ m/s. The radial velocity was measured only at $r = 6$ mm on either side of the burner centerline, since the linear dependency of v on the radius is very well reproducible. The lines in between the actual data points are drawn for clarity. Is appears that the flame is very well symmetric. The small zero shift is caused by small alignment errors in the LDV optics. However, these are of no importance for the temperature calculation, since only the value of c_r is necessary.

It can be seen that below $x = 1$ mm (i.e., in the flame zone) the results for v are probably unreliable. The reason for this is seeding slip, induced by the steep velocity increase in the reaction zone.

It can be concluded that the flat flame behaves well in accordance with the assumptions stated earlier, although the results may possess an uncertainty for low values of U.

Expansion and buoyancy

The effect of buoyancy on the axial velocity is shown in Figure 4a, where measurements of $u(x)$ are presented for $r = 0$, at $x = 0$ to 12 mm, with $U = 0.1$, 0.15 and 0.25 m/s. The acceleration of the burnt gas where ρ is constant, is clearly seen.

Another view on the effect of expansion and buoyancy is obtained from a plot of $c_r(x)$, shown in Figure 4b. For $U = 0.29$ m/s the expansion in the reaction zone can be observed by the positive values of c_r. For lower values of U the expansion is occurring for $x < 1$ mm, where the measurements of v were unreliable. For the temperature

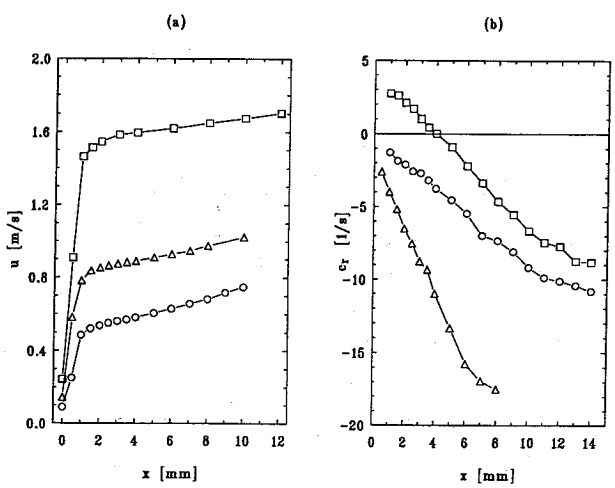

FIGURE 4a, b a. The axial velocity component of the burnt gas u as function of x, at $r = 0$ mm, markers: ○ $U = 0.1$ m/s, △ $U = 0.15$ m/s, □ $U = 0.25$ m/s; b. c_r as function of x, markers: △ $U = 0.1$ m/s, ○ $U = 0.25$ m/s, □ $U = 0.29$ m/s

calculation we assume that $c_r = 0$ for $x = 0$, and obtain values for c_r for $x > 0$ up to the first reliable point by interpolation. Note that over a relatively large distance c_r is approximately linear with x. This will be explained later.

Temperature results

With Figure 4a and 4b all the data are available to calculate the temperature. In Figure 5a some results are shown, for $U = 0.1, 0.15$ and 0.25 m/s, and $\phi = 0.8$. For comparison we used the 1-D flame code, thermodynamic properties and transport data of Kee *et al.* (1986), (1987) and (1991), respectively. The chemical reaction mechanism consisted of 58 reactions between 17 species, as described by Kee *et al.* (1991). As can be seen, good agreement is obtained. Note that for large x the measured temperature is decreasing again due to heat losses to the environment. This may be as large as 10 K/mm. Furthermore, at large distance from the burner plate the LDV measurements are inaccurate, because of oscillations in the burnt gas flow.

We also compared the maximum temperature T_b to results of Kaskan (1967). This is shown in Figure 5b. Also shown is the temperature of the 1-D flame calculations at the same position as where T_b is measured. The results of Kaskan are compiled data of several sources. Therefore we present a best fit of these data (continuous line). It is found that good agreement is obtained. For $U = 0.15$ and 0.2 m/s, where the heat loss of the flame is large, the differences are somewhat larger too, but never more than 70 K. This implies that a burner plate temperature variation of 20 K has still only a small effect on the flame temperature.

For $\phi = 0.8$ the average molar mass is practically constant. We also applied the method to rich mixtures of methane with air, where M is not constant. This can be seen in Figure 6a, where for various values of ϕ the magnitude of $K(x_b)$ is shown. To show

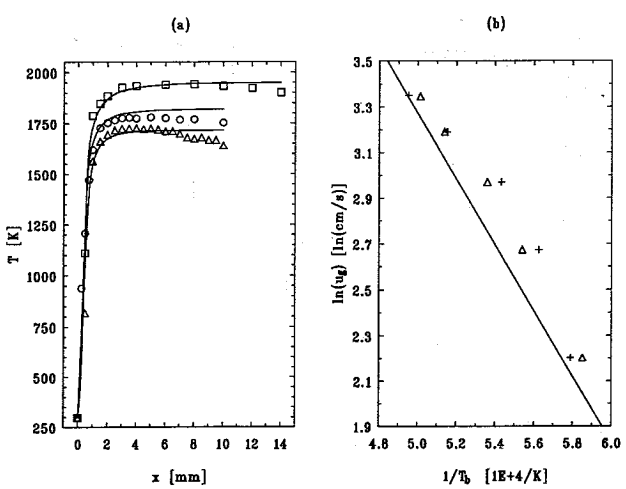

FIGURE 5a, b a. The gas temperature T as function of x, at $r = 0$, markers: $\triangle U = 0.1$ m/s, $\circ U = 0.15$ m/s, $\square U = 0.25$ m/s, lines: 1-D flame calculations; b. The maximum burnt gas temperature T_b as function of u_g markers: + experiments, $\triangle$ 1-D flame calculations line: Kaskan (1967)

(a)

ϕ (-)	M_g (g/mol)	M_b (g/mol)	$K(x_b)$ (-)
0.8	27.85	27.81	1.001
0.9	27.73	27.62	1.004
1.0	27.62	27.38	1.009
1.1	27.51	26.89	1.023
1.2	27.41	26.25	1.044
1.3	27.30	25.72	1.061
1.4	27.17	25.17	1.079

(b)

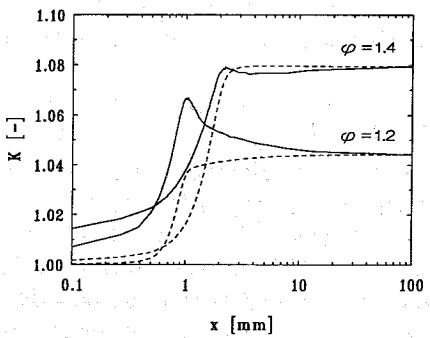

FIGURE 6a, b a. The change of M due to chemical reaction in methane/air mixtures, from 1-D flame calculations; b. The correction factor K, for $\phi = 1.2$, $U = 0.2$ m/s, and $\phi = 1.4$, $U = 0.15$ m/s continuous lines: 1-D flame calculations, dashed lines: Equation (7)

that Equation (6) is indeed a valid approximation, in Figure 6b the result for $K(x)$ with Equation (6) is compared to the result that is obtained using the 1-D flame code, for $\phi = 1.2$ and $U = 0.2$ m/s, and for $\phi = 1.4$ and $U = 0.15$ m/s. It appears that the relative error in K is always less than 2%.

In Figure 7 the temperature profiles are shown for the same two cases. It is compared to 1-D flame calculations and experimental results of Kaskan. It can be seen that despite the correction the results are still very satisfactory.

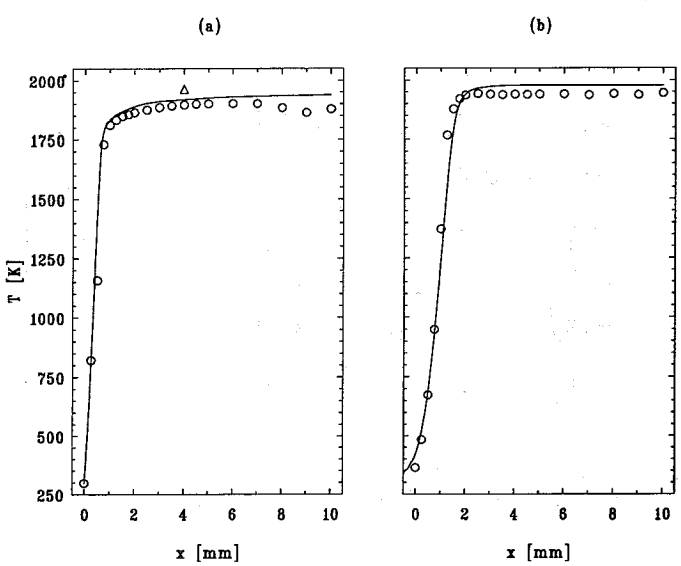

FIGURE 7 The gas temperature T as function of x, at $r = 0$, for rich methane-air mixtures (a) $\phi = 1.2$, $U = 0.2$ m/s; (b) $\phi = 1.4$, $U = 0.2$ m/s, markers: ○ experiments, △ Kaskan (1967), lines: 1-D flame calculations

MODELLING OF BUOYANCY IN THE BURNT GAS FLOW

As can be concluded from the previous section, the method to determine the temperature profile from 2-D velocity measurements gives good results. However, it is still unclear what the relationship is between the gas velocity, the temperature and the burner diameter. It is likely that when the burner diameter is very large, the flat flame will behave as a perfectly 1-D flame, i.e. according to Equation (3). In the case of a very small flame expansion and buoyancy will be predominant.

In order to obtain an estimate for this effect, we derived a simple model for the burnt gas flow. We restrict the analysis to the core region of the flow after the flame, where $u = u(x)$ and $\rho = \rho_b$, and where viscous effects are unimportant. Furthermore, the environment is assumed to have a mass density ρ_0. Then, the conservation of momentum equation in cylindrical coordinates can be written as:

$$u\frac{\partial v}{\partial x} + v\frac{\partial v}{\partial r} = -\frac{1}{\rho}\frac{\partial P}{\partial r} \tag{9}$$

$$u\frac{\partial u}{\partial x} + v\frac{\partial u}{\partial r} = -\frac{1}{\rho}\frac{\partial P}{\partial x} + g\cdot\frac{\rho_0 - \rho}{\rho} \tag{10}$$

Substituting Equation (5), $u = u(x)$ and $\rho = \rho_b$ into Equations (9) and (10), with $g\cdot[\rho_0 - \rho_b]/\rho_b = \mathscr{G}$, yields:

$$-\frac{1}{2}u\frac{\partial^2 u}{\partial x^2} + \frac{1}{4}\left[\frac{\partial u}{\partial x}\right]^2 = -\frac{1}{\rho_b r}\cdot\frac{\partial P}{\partial r} \tag{11}$$

$$u\frac{\partial u}{\partial x} = -\frac{1}{\rho_b}\cdot\frac{\partial P}{\partial x} + \mathscr{G}. \tag{12}$$

If we assume $\partial P/\partial r = 0$, substitution in Equation (11) yields:

$$u\frac{\partial^2 u}{\partial x^2} = \frac{1}{2}\left[\frac{\partial u}{\partial x}\right]^2. \tag{13}$$

Differentiating Equation (13) once more, we obtain:

$$\frac{\partial^3 u}{\partial x^3} = 0 \tag{14}$$

with as general non-trivial solution for $u(x)$ and $v(x)$:

$$u(x) = a_0 + a_1 x + a_2 x^2$$

$$v(x,r) = -\tfrac{1}{2}r\cdot[a_1 + 2a_2 x] \tag{15}$$

with $a_1 = 2\cdot[a_0 a_2]^{1/2}$. It appears that the form of Equation (14) describes the flow of the burnt gas very well. The measured axial velocity deviates typically only 1–2% from Equation (15). Furthermore, in Figure 4b it was seen that c_r is a linear dependent on x.

Nevertheless, the burner geometry or the flame temperature is not included in Equation (14). The reason for this is that in practical flames it is unrealistic that $\partial P/\partial r = 0$, as concluded from Equation (12). Because the flame has a finite diameter,

P must be zero at a certain radius R, e.g., the burner plate radius. Instead of $P = P(x)$ we write $P(x,r)$ to a first order approximation in r as:

$$P(x,r) = p_0(x)\cdot\frac{R^2 - r^2}{R^2} \tag{16}$$

and substitute this into Equations (9) and (10). Taking zero order r-dependence, this yields:

$$-\frac{1}{2}u\frac{\partial^2 u}{\partial x^2} + \frac{1}{4}\left[\frac{\partial u}{\partial x}\right]^2 = \frac{2p_0}{\rho_b R^2} \tag{17}$$

$$u\frac{\partial u}{\partial x} = -\frac{1}{\rho_b}\frac{\partial p_0}{\partial x} + \mathcal{G}. \tag{18}$$

p_0 can be eliminated after integration of Equation (17) with respect to x, to yield a new Equation for u only:

$$-\frac{1}{2}u\frac{\partial^2 u}{\partial x^2} + \frac{1}{4}\left[\frac{\partial u}{\partial x}\right]^2 = \frac{2\mathcal{G}[x - x_1] - u^2 + u_1^2}{R^2} \tag{19}$$

in which we used $u(x_1) = u_1$ as boundary condition. This Equation incorporates the effects of buoyancy and expansion on the velocity of the burnt gas. We will analyze this Equation for the two extreme cases $R \to \infty$ and $R \to 0$.

For $R \to \infty$ Equation (19) reduces to Equation (13), with Equation (15) as solution for u and v. This implies that Equation (15) describes the behavior of the burnt gas of a flame with a relatively large diameter. For $R \to 0$ it is found that Equation (19) reduces to:

$$u^2 - u_1^2 = 2\mathcal{G}\cdot[x - x_1]. \tag{20}$$

This result would also be obtained when Equation (12) is solved with $\partial P/\partial x = 0$ (no pressure terms induced by expansion). Equation (20) can be interpreted as the effect of buoyancy alone on the burnt gas, where the mass density difference predominantly determines the burnt gas acceleration. Because the acceleration is small, Equation (20) can be approximated by:

$$u(x) \simeq u_1 + \frac{\mathcal{G}}{u_1}\cdot[x - x_1] \tag{21}$$

showing the constant acceleration of a mass experiencing a constant force.

In a practical flame, with R neither zero nor infinite, the behavior will be somewhere in between the two extremes of Equations (15) and (20). Therefore, with Equation (20) we define a "buoyancy index" β as:

$$\beta = \frac{u^2 - u_1^2}{2\mathcal{G}\cdot[x - x_1]}. \tag{21}$$

For $R \to 0$ it follows that $\beta = 1$, while $\beta = 0$ for $R \to \infty$. This means that the magnitude of β indicates whether large or small flame behavior is found for a certain burner and

TABLE I

The Buoyancy Index β for Various Values of U

U(m/s)	Burner diameter	
	20 mm	30 mm
0.07	–	0.28
0.09	–	0.28
0.10	0.41	–
0.15	0.44	0.32
0.20	0.46	0.34
0.25	0.33	0.37
0.29	–	0.29

flame situation. In Table 1 some values for β are given, for measurements with a 20 mm and a 30 mm burner. It appears that β is about 0.3 and 0.4, respectively, which means that Equation (15) must be the dominant solution. This is in accordance with the earlier statement about the case $R \to \infty$.

The small difference between β for a 20 and a 30 mm burner suggests, that $\beta \to 0$ is achieved only for burners with a radius considerably larger than 30 mm.

CONCLUSIONS

The perforated plate burner is a useful tool for investigating laminar flat flames. It produces flames with uniform velocity profiles when the unburnt gas velocity is low or near the adiabatic burning velocity.

Laser Doppler Velocimetry measurements have shown that due to expansion (in the reaction zone of the flame) and buoyancy a non-zero radial velocity component is inherent to flat flames.

A new method is presented with which the temperature profile of the flame can be derived from two-dimensional velocity measurements. The results are in close agreement with both one-dimensional flame calculations and experimental data in the literature.

A simple model of the burnt gas flow qualitatively describes the influence of expansion and buoyancy on the velocity, in relation with the flame temperature and the burner diameter. It can be used to asses the relative importance of expansion and buoyancy in relation to the burner diameter and the flame temperature. More experiments performed with larger burners (> 30 mm diameter) are needed to confirm the validity of the model.

ACKNOWLEDGEMENTS

The support of Gastec N.V. and NOVEM, the Netherlands, is gratefully acknowledged. The authors would also like to thank P.J.A.G. Weijtmans, who performed some of the measurements.

REFERENCES

Botha, J. P. and Spalding, D. B. (1954). The laminar flame speed of propane/air mixtures with heat extraction from the flame. *Proc. Roy. Soc. A.*, **225**, 71.

Fox, J. S. and Kihara, D. H. (1972). Temperature non-uniformity in a porous disk burner. *Combus Sci and Tech.*, **5**, 17.

de Goey, L. P. H., van Maaren, A. and Quax, R. M. (1993). Stabilization of adiabatic premixed laminar flames on a flat flame burner. *Combus. Sci. and Tech.*, **92**, 201–207.

Kaskan, W. E. (1967). The dependence of flame temperature on mass burning velocity. *6th Symposium (int.) on Combustion*, the Combustion Institute, Pittsburg, 134.

Kee, R. J. *et al.* (1991). *A Fortran program for modelling steady laminar one-dimensional premixed flames.* Sandia report SAND85-8240. UC-401. Sandia National Laboratories, Livermore, California 94551, U.S.A.

Kee, R. J. *et al.* (1987). *The Chemkin thermodynamic data base.* Sandia Report SAND87-8215B.UC-4. Sandia National Laboratories, Livermore, California 94551, U.S.A.

Kee, R. J. *et al.* (1986). *A Fortran computer code package for the evaluation of gasphase multicomponent transport properties.* Sandia Report SAND86-8246.UC-401. Sandia National Laboratories, Livermore, California 94551, U.S.A.

Kihara, D. H., Fox, J. S. and Kinoshita, C. M. (1975). Temperature and velocity non-uniformity in edge cooled flat flame burners. *Combus. Sci. and Tech.*, **11**, 239.

van Maaren, A., Thung, D. S. and de Goey, L. P. H. (1993). Measurement of flame temperature and adiabatic burning velocity of methane/air mixtures. (*to appear in Combustion Science and Technology*).

Pritchard, R. *et al.* (1972) Diameter effects in cooled flat-flame burners. *Combustion and Flame*, **18**, 13.